The chemistry of graphene oxide

Daniel R. Dreyer,[a] Sungjin Park,[b] Christopher W. Bielawski*[a] and Rodney S. Ruoff*[b]

Received 7th October 2009
First published as an Advance Article on the web 3rd November 2009
DOI: 10.1039/b917103g

The chemistry of graphene oxide is discussed in this *critical review*. Particular emphasis is directed toward the synthesis of graphene oxide, as well as its structure. Graphene oxide as a substrate for a variety of chemical transformations, including its reduction to graphene-like materials, is also discussed. This review will be of value to synthetic chemists interested in this emerging field of materials science, as well as those investigating applications of graphene who would find a more thorough treatment of the chemistry of graphene oxide useful in understanding the scope and limitations of current approaches which utilize this material (91 references).

1. Introduction

During the last half decade, chemically modified graphene (CMG) has been studied in the context of many applications, such as polymer composites, energy-related materials, sensors, 'paper'-like materials, field-effect transistors (FET), and biomedical applications, due to its excellent electrical, mechanical, and thermal properties.[1,2] Chemical modification of graphene oxide, which is generated from graphite oxide (GO, see below for structure(s) and production methods), has been a promising route to achieve mass production of CMG platelets. Graphene oxide contains a range of reactive oxygen functional groups, which renders it a good candidate for use in the aforementioned applications (among others) through chemical functionalizations. We recommend that interested readers take note of recent review papers about the physical properties of graphene,[1] and separately, chemical methods to produce CMGs *via* established colloidal suspension methodologies.[2] This *critical review* will focus on the chemistry of graphene oxide, including its preparation, structure, and reactivity. The reactions described below are classified into (i) reductions (removing oxygen groups from graphene oxide) and (ii) chemical functionalizations (adding other chemical functionalities to graphene oxide).

[a] *Department of Chemistry and Biochemistry, The University of Texas at Austin, 1 University Station, A5300, Austin, TX, 78712, USA. E-mail: bielawski@cm.utexas.edu; Fax: +1 512-471-5884; Tel: +1 512-232-3839*
[b] *Department of Mechanical Engineering, Texas Materials Institute, The University of Texas at Austin, 204 E. Dean Keeton St., Austin, TX, 78712, USA. E-mail: r.ruoff@mail.utexas.edu; Fax: +1 512-471-7681; Tel: +1 512-471-4691*

2. Synthesis and structural characterization of GO

2.1 Synthetic approaches

Despite the relative novelty of graphene as a material of broad interest and potential,[1,3] GO has a history that extends back many decades to some of the earliest studies involving the chemistry of graphite.[4–6] The first, well-known example came

Daniel R. Dreyer

Daniel R. Dreyer is a PhD candidate in organic chemistry at The University of Texas at Austin studying under Prof. Christopher W. Bielawski. He received his BS in chemistry from Wheaton College (IL) in 2007 where he conducted research in confocal microscopy under Prof. Daniel L. Burden. During his undergraduate career he also studied X-ray reflectometry and plasma polymerization under Prof. Mark D. Foster at the University of Akron as part of an NSF-sponsored REU. His current research interests include applications of ionic liquids in synthetic polymer chemistry, structurally dynamic/self-healing materials, and novel electrolytes for graphene-based energy storage devices.

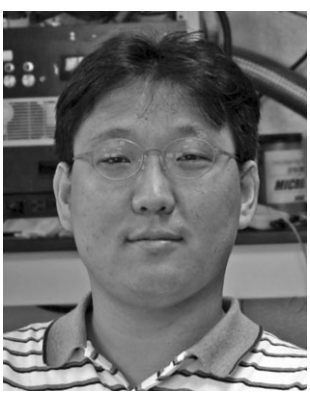

Sungjin Park

Sungjin Park received his PhD in 2005 under the tutelage of Prof. Youngkyu Do at KAIST, South Korea, developing catalysts for olefin polymerization. Following his graduate studies, he moved to the laboratory of Prof. Insung S. Choi at KAIST, studying carbon nanotube-based chemistry and composites and surface chemistry, then joined the research groups of Profs. Rodney S. Ruoff and SonBinh T. Nguyen at Northwestern University and began studying graphene-based materials and their chemistry. In 2007, he followed Prof. Ruoff to The University of Texas at Austin, where he is currently a postdoctoral scholar.

in 1859 when British chemist B. C. Brodie was exploring the structure of graphite by investigating the reactivity of flake graphite. One of the reactions he performed involved adding "potash of chlorate" (potassium chlorate; $KClO_3$) to a slurry of graphite in fuming nitric acid (HNO_3).[7] Brodie determined that the resulting material was composed of carbon, hydrogen, and oxygen, resulting in an increase in the overall mass of the flake graphite. He isolated crystals of the material, but the interfacial angles of the crystal lattice were unable to be measured *via* reflective goniometry. Successive oxidative treatments resulted in a further increase in the oxygen content, reaching a limit after four reactions. The C : H : O composition was determined to be 61.04 : 1.85 : 37.11; a net molecular formula of $C_{2.19}H_{0.80}O_{1.00}$. Brodie found the material to be dispersible in pure or basic water, but not in acidic media, which prompted him to term the material "graphic acid." After heating to a temperature of 220 °C, the C : H : O composition of this material changed to 80.13 : 0.58 : 19.29 ($C_{5.51}H_{0.48}O_{1.00}$), coupled with a loss of carbonic acid and "carbonic oxide."

Throughout his studies, Brodie was interested in the molecular formula of "graphite" and its discrete molecular weight. Ultimately, he determined the molecular weight of graphite to be 33, saying:

"*This form of carbon should be characterized by a name marking it as a distinct element. I propose to term it Graphon.*"

Nearly 150 years later, "graphene" would take the physics and chemistry communities by storm.

We now know that Brodie was mistaken in his search for a discrete molecular formula for graphite, and the indeterminate nature of this material shall be discussed more fully in the following sections. Nearly 40 years after Brodie's seminal discovery of the ability to oxidize graphite, L. Staudenmaier improved Brodie's $KClO_3$-fuming HNO_3 preparation by adding the chlorate in multiple aliquots over the course of the reaction (also, with the addition of concentrated sulfuric acid, to increase the acidity of the mixture), rather than in a single addition as Brodie had done. This slight change in the procedure resulted in an overall extent of oxidation similar to Brodie's multiple oxidation approach (C : O ~ 2 : 1), but performed more practically in a single reaction vessel.[8]

Nearly 60 years after Staudenmaier, Hummers and Offeman developed an alternate oxidation method by reacting graphite with a mixture of potassium permanganate ($KMnO_4$) and concentrated sulfuric acid (H_2SO_4), again, achieving similar levels of oxidation.[9] Though others have developed slightly modified versions, these three methods comprise the primary routes for forming GO, and little about them has changed. Importantly, it has since been demonstrated that the products of these reactions show strong variance, depending not only on the particular oxidants used, but also on the graphite source and reaction conditions. This point will be borne out in the discussions that follow. Because of the lack of understanding of the direct mechanisms involved in these processes, it is instructive to consider examples of the reactivities of these chemicals in other, more easily studied, systems. The Brodie and Staudenmaier approaches both use $KClO_3$ and nitric acid (most commonly fuming [> 90% purity]) and will be treated together.

Nitric acid is a common oxidizing agent (*e.g.* aqua regia) and is known to react strongly with aromatic carbon surfaces, including carbon nanotubes.[10,11] The reaction results in the formation of various oxide-containg species including carboxyls, lactones, and ketones. Oxidations by HNO_3 result in the liberation of gaseous NO_2 and/or N_2O_4 (as demonstrated in Brodie's observation of yellow vapors).[12] Likewise, potassium chlorate is a strong oxidizing agent commonly used in blasting caps or other explosive materials. $KClO_3$ typically is an *in situ* source of dioxygen, which acts as the reactive species.[12] These were among the strongest oxidation conditions known at the time, and continue to be some of the strongest used on a preparative scale.

The Hummers method uses a combination of potassium permanganate and sulfuric acid. Though permanganate is a commonly used oxidant (*e.g.* dihydroxylations), the active species is, in fact, diamanganese heptoxide (Scheme 1). This

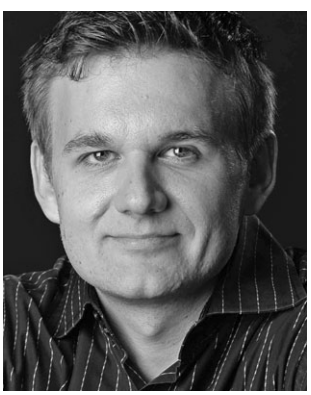

Christopher W. Bielawski

Christopher W. Bielawski received a BS degree in Chemistry from the University of Illinois at Urbana-Champaign (1996) and a PhD in Chemistry from the California Institute of Technology (2003). After postdoctoral studies (also at Caltech), he became an assistant professor of chemistry at The University of Texas at Austin in 2004 and was promoted to associate professor in 2009. Prof. Bielawski's research program lies at the interface of polymer, synthetic organic, and organometallic chemistry.

Rodney S. Ruoff

Rod Ruoff is a Cockrell Family Regents Chair at The University of Texas at Austin, after having been Director of the Biologically Inspired Materials Institute at Northwestern University. He received his BS in Chemistry from UT-Austin and PhD in Chemical Physics from the UI-Urbana (advisor HS Gutowsky). Prior to Northwestern he was a Staff Scientist at the Molecular Physics Laboratory of SRI International and Associate Professor of Physics at Washington University. He has 205 refereed journal articles in the fields of chemistry, physics, mechanics, & materials science, and is a co-founder of Graphene Energy Inc., and founder of Nanode, Inc.

$$KMnO_4 + 3\,H_2SO_4 \longrightarrow K^+ + MnO_3^+ + H_3O^+ + 3\,HSO_4^-$$

$$MnO_3^+ + MnO_4^- \longrightarrow \mathbf{Mn_2O_7}$$

Scheme 1 Formation of dimanganeseheptoxide (Mn_2O_7) from $KMnO_4$ in the presence of strong acid (adapted from ref. 13).

dark red oil is formed from the reaction of potassium permanganate with sulfuric acid. The bimetallic heptoxide is far more reactive than its monometallic tetraoxide counterpart, and is known to detonate when heated to temperatures greater than 55 °C or when placed in contact with organic compounds.[13,14] Trömel and Russ demonstrated the ability of Mn_2O_7 to selectively oxidize unsaturated aliphatic double bonds over aromatic double bonds, which may have important implications for the structure of graphite and reaction pathway(s) occuring during the oxidation (see below).[15]

The most common source of graphite used for chemical reactions, including its oxidation, is flake graphite, which is a naturally occuring mineral that is purified to remove heteroatomic contamination.[16] As such, it contains numerous, localized defects in its π-structure that may serve as seed points for the oxidation process. If Trömel and Russ's observations on styrene can be applied to graphite, then it is likely that the oxidation observed is not that of aromatic systems, but rather of isolated alkenes. The complexity of flake graphite, and the defects that are inherent as a result of its natural source, make the elucidation of precise oxidation mechanisms very challenging, unfortunately. Few other oxidants have been used for the formation of GO, though Jones' reagent (H_2CrO_4/H_2SO_4) is commonly used for the formation of expanded graphite, whose partially oxidized, intercalated structure is somewhere between graphite and true graphite oxide.[17] The recent review by Wissler is an excellent, succinct source of further information on commonly used graphites and carbons, as well as the terminology used to describe these materials.[16]

2.2 Structural features

Aside from the operative oxidative mechanisms, the precise chemical structure of GO has been the subject of considerable debate over the years, and even to this day no unambiguous model exists. There are many reasons for this, but the primary contributors are the complexity of the material (including sample-to-sample variability) due to its amorphous, berthollide character (*i.e.* nonstoichiometric atomic composition) and the lack of precise analytical techniques for characterizing such materials (or mixtures of materials). Despite these obstacles, considerable effort has been directed toward understanding the structure of GO, much of it with great success.

Many of the earliest structural models of GO proposed regular lattices composed of discrete repeat units. Hofmann and Holst's stucture (Fig. 1) consisted of epoxy groups spread across the basal planes of graphite, with a net molecular formula of C_2O.[18] Ruess proposed a variation of this model in 1946 which incorporated hydroxyl groups into the basal plane, accounting for the hydrogen content of GO.[19] Ruess's model also altered the basal plane structure to an sp^3 hybridized system, rather than the sp^2 hybridized model of Hofmann and Holst. The Ruess model still assumed a repeat unit, however, where $\frac{1}{4}$th of the cyclohexanes contained epoxides in the 1,3 positions and were hydroxylated in the 4 position, forming a regular lattice structure. This was supported by Mermoux based on observed structural similarities to poly(carbon monofluoride), $(CF)_n$,[20] a structure that entails the formation of C–F bonds through the complete rehybridization of the sp^2 planes in graphite to sp^3 cyclohexyl structures.[21] In 1969, Scholz and Boehm suggested a model that completely removed the epoxide and ether groups, substituting regular quinoidal species in a corrugated backbone.[22] Another remarkable model by Nakajima and Matsuo relied on the assumption of a lattice framework akin to poly(dicarbon monofluoride), $(C_2F)_n$, which forms a stage 2 graphite intercalation compound (GIC).[23] These individuals also made a valuable contribution to understanding the chemical nature of GO by proposing a stepwise mechanism for its formation *via* 3 of the more common oxidation protocols.[24]

The most recent models of GO have rejected the lattice-based model and have focused on a nonstoichiometric, amorphous alternative. Certainly the most well-known model is the one by Lerf and Klinowski (Fig. 2). Anton Lerf and Jacek Klinowski have published several papers on the structure and hydration behavior of GO, and these are the most widely cited in the contemporary literature. The initial studies done by Lerf and coworkers used solid state nuclear

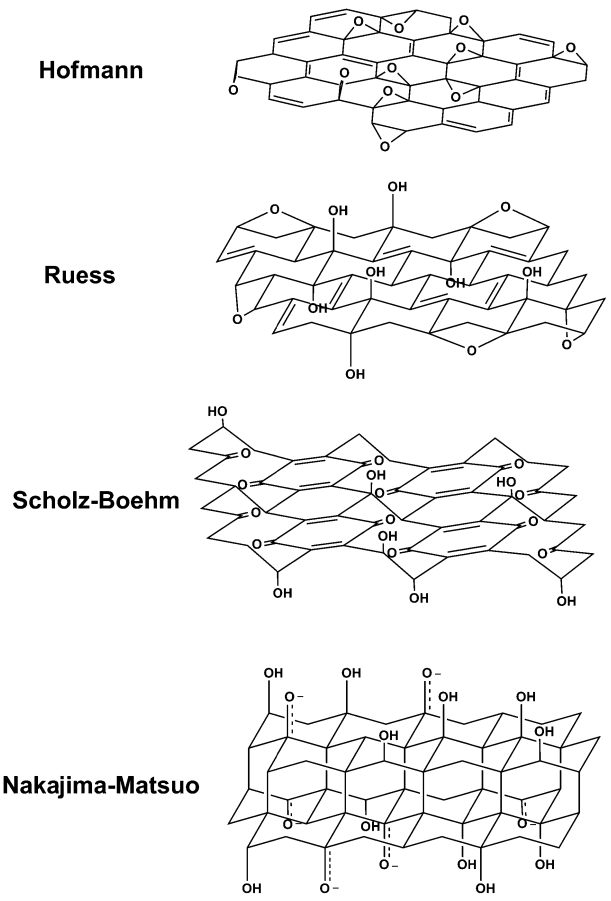

Fig. 1 Summary of several older structural models of GO (adapted from ref. 27).

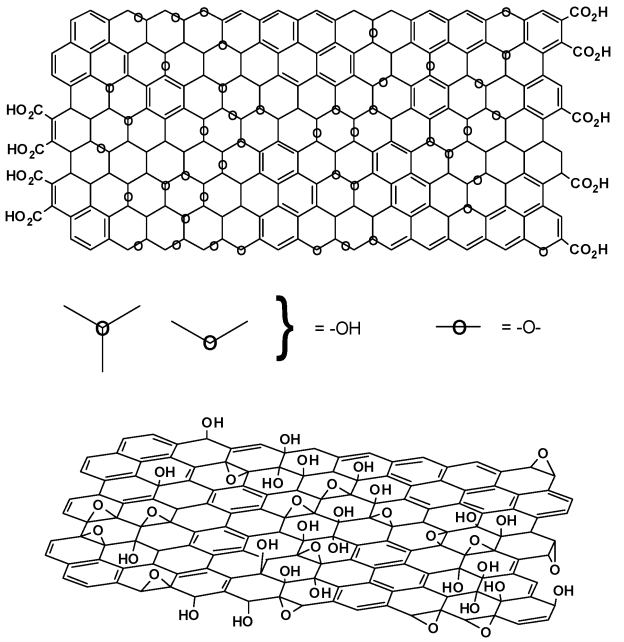

Fig. 2 Variations of the Lerf-Klinowski model indicating ambiguity regarding the presence (top, adapted from ref. 26) or absence (bottom, adapted from ref. 34) of carboxylic acids on the periphery of the basal plane of the graphitic platelets of GO.

magnetic resonance (NMR) spectroscopy to characterize the material.[25] This was a first for the field as earlier models relied primarily on elemental composition, reactivity and X-ray diffraction studies. By preparing a series of GO derivatives, Lerf was also able to isolate structural features based on the material's reactivity.[26]

Cross polarization/magic angle spinning (CP/MAS) experiments displayed three broad resonances at 60, 70 and 130 ppm in the ^{13}C NMR spectrum of GO. Short-contact-time spectra display only signals at δ = 60 and 70 ppm. Using Mermoux's model to show that all carbons in GO are quaternary,[20] the peak at 60 ppm was assigned to tertiary alcohols, the peak at 70 ppm to epoxy (1,2-ether) groups, and the peak at 130 ppm to a mixture of alkenes. Short-contact-time experiments also showed that there was significant inter-platelet hydrogen bonding through the alcohols and epoxide functional groups, contributing significantly to the stacked structure of GO. These results were in good agreement with the overall functional group identity of the older models (with the exception of proposing 1,2-ethers instead of 1,3-ethers[27]), but questions remained as to the distribution of these functionalities. In particular, were the alkenes isolated from one another, or were they clustered in either aromatic or conjugated clusters? The answer to this question would have important ramifications for the electronic structure and chemical reactivity of GO.

To address this problem, Lerf and coworkers reacted GO with maleic anhydride,[25] which is a good dienophile for [4 + 2] (Diels–Alder type) cycloaddition reactions. Conjugated, non-aromatic alkenes should readily react with this substrate. Both the ^{1}H and ^{13}C spectra were virtually identical to the starting material, however, suggesting that no reaction had occurred; results that were largely inconclusive.

However, treatment of GO with D_2O eliminated the water peak in the respective ^{1}H NMR spectrum, allowing for resolution of proton signals buried beneath the intense resonance caused by water bound to the surface of GO. The signal attributed to the tertiary alcohols (δ = 1.3 ppm) was not significantly affected, indicating a slower exchange process, relative to the water molecules intercalated into the interlayer of GO. A second peak at δ = 1.0 ppm was observed, however, indicative of the presence of at least two magnetically inequivalent alcohol species. The exact identity of this/these species remains unknown, but it is reasonable to surmise that it is reflective of strong hydrogen bonding interactions either to water intercalated between the platelets or to other platelets. Reaction with sodium ethoxide also demonstrated the ability to use the epoxides as electrophilic centers for surface functionalization.[25,28] Collectively, these data indicate that the dominant structural features present on the surface of GO are tertiary alcohols and ethers, most likely 1,2-ethers (*i.e.* epoxides). These conclusions have been the basis for a variety of reactivity studies, and will be discussed more fully in the sections to come.

In these early NMR studies, it was noted that full-width-at-half-maximum height of the water peak remains nearly constant in the ^{1}H NMR spectrum (approx. 2.8 kHz) across a wide temperature (123–473 K), indicating very strong interactions between the water and the GO.[28] This is likely a key factor in maintaining the stacked structure of GO. The behavior of water in GO has also been characterized by neutron scattering, confirming the water is strongly bound to the basal plane of GO through hydrogen bonding interactions with the oxygen in the epoxides of the GO (Fig. 3).[29–31]

While the studies mentioned above outlined many of the fundamental structural features of GO, a more refined picture of the complexity of the material was necessary. Lerf and coworkers proceeded by reacting GO with a range of reactive species.[26] They determined that the double bonds were likely either aromatic or conjugated, the logic being that isolated double bonds would be unlikely to persist in the strong oxidizing conditions used (a modified Hummers method). This revised Lerf–Klinowski model also incorporated the infrared spectroscopic data from decades earlier indicating that

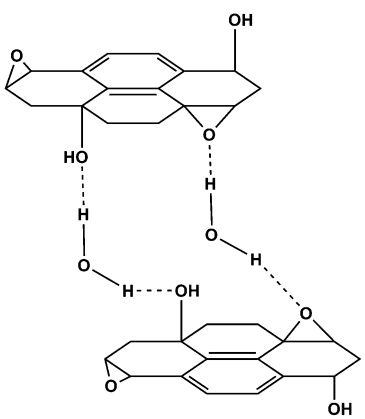

Fig. 3 Proposed hydrogen bonding network formed between oxygen functionality on GO and water. For alternatives to this model see ref. 26 and 28.

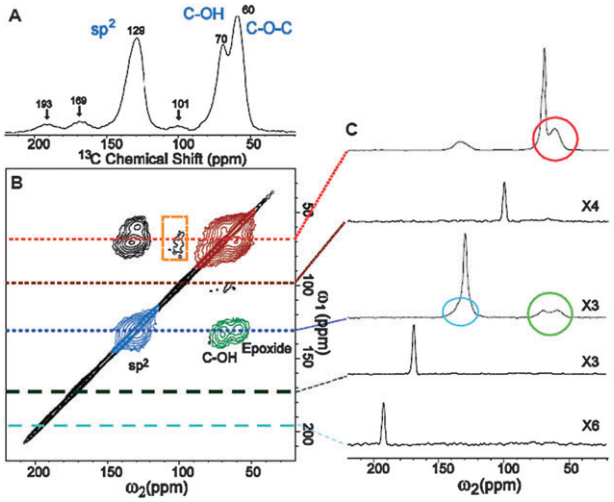

Fig. 4 (A) 1D ^{13}C MAS and (B) 2D $^{13}C/^{13}C$ chemical-shift correlation solid-state NMR spectra of ^{13}C-labeled GO with (C) slices selected from the 2D spectrum at the indicated positions (70, 101, 130, 169, and 193 ppm) in the ω_1 dimension. The green, red, and blue areas in (B) and circles in (C) represent cross peaks between sp^2 and C–OH/epoxide carbons (green), those between C–OH and epoxide carbons (red), and those within sp^2 groups (blue), respectively (from ref. 36).

carboxylic acid groups were present in very low quantities at the periphery of the graphitic platelets, in addition to other keto groups.[22,32,33] The key features of this model are summarized in Fig. 2.

As Brodie observed in 1859, along with many others since, Lerf and coworkers noted the thermal instability of GO. After calcinating in a vacuum at 100 °C, the signals found at $\delta = 60$ and 70 ppm in the ^{13}C NMR spectrum of the resulting material disappeared, leaving only a signal at 122 ppm. They attributed this signal to the presence of aromatic and phenolic (or aromatic diol) species.[34]† The decomposition process (discussed in greater detail below) is known to involve the evolution of CO and CO_2, rather than O_2, due to the high surface reactivity of GO itself.[35] Thermal decomposition (in ambient atmosphere) at higher temperatures was reported to result in a highly-disordered mixture of various oxygen-containing graphitic carbons that are difficult to characterize. Though the Lerf–Klinowski model remains largely unchanged since its initial report over 10 years ago, others have made slight modifications to the proposed structure including the presence of 5- and 6-membered lactols on the periphery of the graphitic platelets as well as the presence of esters of the tertiary alcohols on the surface, though all accounts maintain the dominance of epoxides and alcohols on the basal plane.[36,37] Cai *et al.* have also recently demonstrated the ability to isotopically label GO, greatly expanding the scope of potential spectroscopic techniques that may be applied to the study of its structure (Fig. 4).[36]

One notable exception to this adherence to the Lerf–Klinowski model has been proposed by Dékány and coworkers (Fig. 5).[27] The Dékány model work revived and

† Notably, this most recent model proposed by Lerf, Klinowski and coworkers does not include the carboxylic acid groups proposed earlier and supported by IR data.[22,32,33]

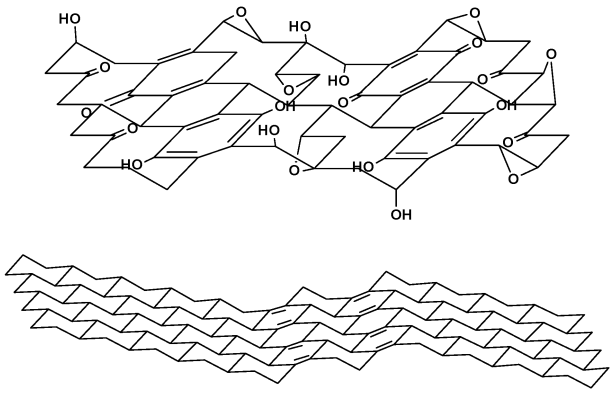

Fig. 5 Structure of GO proposed by Dékány and coworkers (adapted from ref. 27).

updated the Ruess and Scholz–Boehm models, which suggested a regular, corrugated quinoidal structure interrupted by *trans*-linked cyclohexyl regions, functionalized by tertiary alcohols and 1,3-ethers. Reevaluation of the FTIR features of GO, as well as examination by DRIFT spectroscopy,[38] suggested that the signal found at 1714 cm^{-1} in the IR spectrum of this material was not indicative of carboxylic acids, but rather of single ketones and/or quinones. However, potentiometric acid–base titrations indicated the presence of acidic sites on the basal plane of GO.[39] To explain this apparent discrepancy, the Lerf–Klinowski model necessitates a keto-enol isomerization of α,β-unsaturated ketones generated *in situ*, with the enol form providing the proton exchange site. The keto form is thermodynamically more favored, however, disfavoring enolization and acidic proton exchange. However, if the enols are present in aromatic regions (*e.g.* phenol–quinone exchange), the phenoxide is the thermodynamic product and therefore should allow for proton exchange.

In light of these results, the Dékány model is composed of two distinct domains: *trans*-linked cyclohexyl species interspersed with tertiary alcohols and and 1,3-ethers, and a corrugated network of keto/quinoidal species. No carboxylic acids are believed to be present in this description of GO. Further oxidation destroys the alkenes of the quinones through formation of 1,2-ethers, as well as any pockets of aromaticity that may have persisted during the initial oxidative conditions used for its synthesis. It is also hypothesized that the quinones introduce rigidity and plane boundaries, and are a possible source of the macroscopic wrinkling of the platelets commonly seen in TEM images.[27]

As a final note, variations in the degree of oxidation caused by differences in starting materials (principally the graphite source) or oxidation protocol can cause substantial variation in the structure and properties of the material, rendering the term "graphite oxide" somewhat fluid, and subject to misinterpretation. This experimental observation has been compared with density functional calculations, which predict that partial oxidation is thermodynamically favored over complete oxidation.[40] However, the exact identity and distribution of oxide functional groups depends strongly on the extent of coverage. This is illustrated in the theoretical prediction that the ratio of epoxides to alcohols increases with increasing oxidation.[40]

3. Chemical reactivity

3.1 Reductions

Both GO and graphene oxide are electrically insulating materials due to their disrupted sp^2 bonding networks. Because electrical conductivity can be recovered by restoring the π-network, one of the most important reactions of graphene oxide is its reduction. The product of this reaction has been given a variety of names, including: reduced graphene oxide (r-GO), chemically-reduced graphene oxide (CReGO), and graphene. For the sake of clarity, we will refer to the product as "reduced graphene oxide," though the distinction with pristine graphene will be made apparent. The two are often confused but the structural differences can be significant, making the use of separate terms appropriate.

Hitherto we have referred to oxidized graphite as "graphite oxide" (GO). As was discussed in the previous section, this material contains myriad oxide functionalities (predominately alcohols and epoxides), but retains a stacked structure similar to graphite, albeit with much wider spacing (6–12 Å, depending on the humidity) due to water intercalation.[29] In discussing the reduction of this material, however, we must distinguish "graphene oxide" from graphite oxide. Chemically, graphene oxide is similar, if not identical, to GO, but structurally it is very different. Rather than retaining a stacked structure, the material is exfoliated into monolayers or few-layered stacks. The surface functionality (particularly in basic media) greatly weakens the platelet–platelet interactions, owing to its hydrophilicity. A variety of thermal and mechanical methods can be used to exfoliate GO to graphene oxide, though sonicating and/or stirring GO in water are the most common. Sonicating in water or polar organic media, despite being much faster than mechanical stirring, has a great disadvantage in that it causes substantial damage to the graphene oxide platelets.[41] Rather than having a mean size on the order of several microns per side, the dimensions are diminished to several hundred nanometers per side, and the product contains a considerably larger distribution of sizes.[42–44] The oxidation process itself also causes breaking of the graphitic structure into smaller fragments.[45,46]

The maximum dispersibility of graphene oxide in solution, which is important for processing and further derivatization, depends both on the solvent and the extent of surface functionalization imparted during oxidation (Fig. 6); to date it has been found that the greater the polarity of the surface, the greater the dispersability. Dispersabilities are typically on the order of 1–4 mg mL^{-1} in water.[47]‡ Based on AFM studies of graphene oxide platelets collected from these dispersions, it is believed that sonication results in near-complete exfoliation of the GO.[42]

The reduction process is among the most important reactions of graphene oxide, to date, because of the similarities between reduced graphene oxide and pristine graphene. For scientists and engineers endeavoring to use graphene in large scale applications, such as energy storage, chemical conversion of graphene oxide is the most obvious and desirable route (at this time) to large quantities of graphene-like materials. These reduction methods can be achieved through chemical, thermal, or electrochemical reduction pathways. All of these lead to products that resemble pristine graphene to varying degrees (some very closely), particularly in terms of their electrical, thermal, and mechanical properties, as well their surface morphology.

3.1.1 Chemical reduction. When colloidally dispersed, a variety of chemical means may be used to reduce graphene oxide. Certainly the most common and one of the first to be reported was hydrazine monohydrate (Fig. 7).[48] While most strong reductants have slight to very strong reactivity with water, hydrazine monohydrate does not, making it an attractive option for reducing aqueous dispersions of graphene oxide. Reduction of graphene oxide with extremely strong reducing agents, such as lithium aluminium hydride (LAH), remains a challenge due to side reactions with solvents commonly used for dispersing graphene oxide (*i.e.* water). The most straightforward goal of any reduction protocol is to produce graphene-like materials similar to the pristine graphene achieved from direct mechanical exfoliation (*i.e.* the "Scotch tape method") of individual layers of graphite.[49]

Although it remains unclear as to how hydrazine reacts with graphene oxide to afford its reduced counterpart (at least one mechanistic route has been proposed;[48]Scheme 2), the product has been characterized extensively. Combined with a knowledge of hydrazine's reduction pathway in other organic systems, we can make educated guesses for the case of graphene oxide. Hydrazine monohydrate, and a structurally similar species, diimide, are relatively mild reagents commonly used for the selective reduction of alkenes.[50] This process typically occurs through *syn* addition of H_2 across the alkene, coupled with the extrusion of nitrogen gas. Such a process is gentle enough to leave other functionalities, such as cyano and nitro groups, untouched.

There are a handful of useful experiments for characterizing the properties of the resulting, reduced material, as well as the starting material. First is a meaurement of the BET surface area, so named after S. Brunauer, P. H. Emmett, and E. Teller. In short, this experiment quantifies the surface area of a material by measuring the amount of gas (most commonly nitrogen) physisorbed to a surface.[51] Other techniques of value include Raman spectroscopy, where the D (associated with the order/disorder of the system) and G (an indicator of the stacking structure) bands are the dominant vibrational modes observed in graphitic structures. The ratio of the intensities of the two bands (D/G) is often used as a means of determining the number of layers in a graphene sample and its overall stacking behavior; high D/G ratios indicate a high degree of exfoliation/disorder.[52] Also of interest are the electronic properties of the material.

$$R_{sh} = \frac{1}{\sigma t} \quad (1)$$

Most commonly these are expressed as a bulk conductivity (σ; S m^{-1}), but other related values such as sheet resistance (R_{sh}; Ω $sq.^{-1}$) and sheet conductance (G_{sh}; S $sq.^{-1}$) are also reported. Sheet resistance is a measure of the electrical

‡ See a previous review for a comprehensive table of dispersabilities achieved *via* various oxidation procedures.[2]

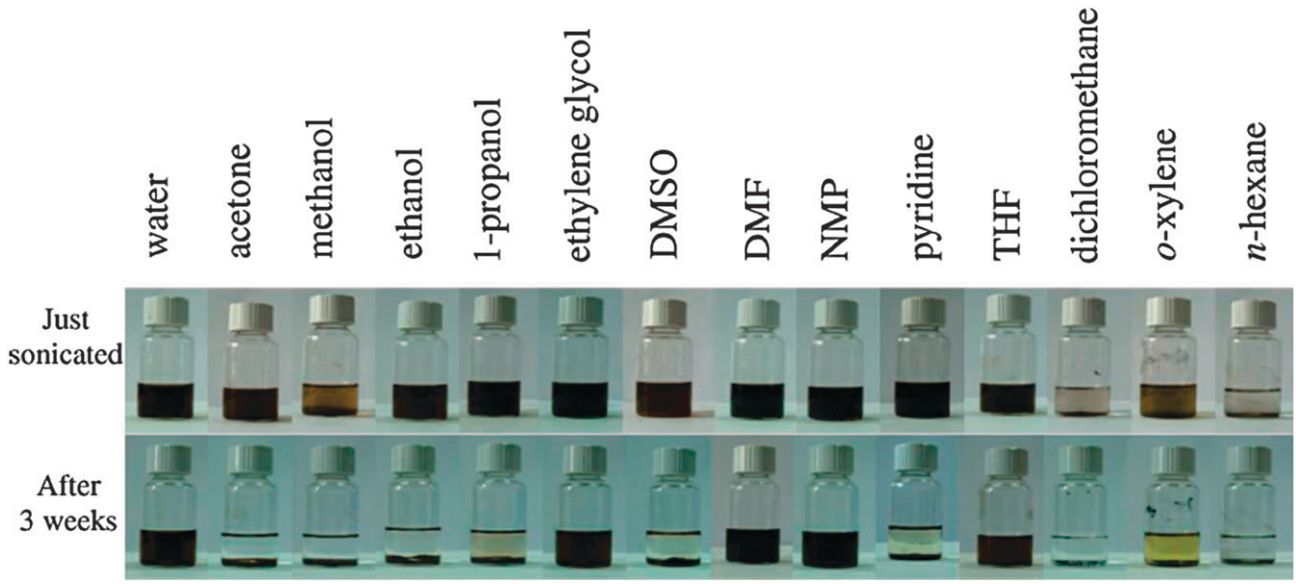

Fig. 6 Digital pictures of as-prepared GO dispersed in water and 13 organic solvents through ultrasonication (1 h). Top: dispersions immediately after sonication. Bottom: dispersions 3 weeks after sonication. The yellow color of the *o*-xylene sample is due to the solvent itself (from ref. 41).

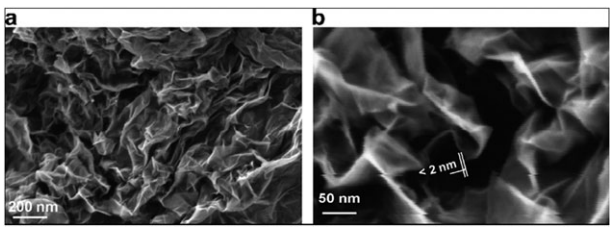

Fig. 7 (a) An SEM image of aggregated reduced graphene oxide platelets. (b) A platelet having an upper bound thickness at a fold of 2 nm. At the resolution limit of the FEG SEM used here, the following are relevant parameters of the microscope and of the specimen. Of the microscope: spot size and flux of e-beam (e-current, density, solid angle/aperture size), energy of the electrons in the primary beam, electromagnetic lens alignment, type of detectors used and their operating parameters. Of the sample: geometry (such as edges, roughness, thickness, and orientation with respect to e-beam), material (such as density, atomic number, electrical conductivity, and composition), substrate or matrix (what the specimen is affixed to or a part of). There is also the role of the operator expertise. Thus for (b) and discussion of a measured value for the fold thickness of about 2 nm, the authors suggest a confidence limit of roughly ±1 nm (from ref. 48).

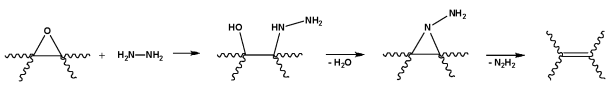

Scheme 2 A proposed reaction pathway for epoxide reduction by hydrazine (adapted from ref. 48).

resistance of the sheet, independent of its thickness. It is related to bulk conductivity by eqn (1), where σ is the bulk conductivity and t is the sample thickness. Numerous other techniques, such as atomic force microscopy (AFM, Fig. 9), X-ray photoelectron spectroscopy (XPS, Fig. 8), scanning electron microscopy (SEM, Fig. 7), and transmission electron microscopy (TEM) are also used, but for the sake of brevity we direct the reader to other sources on these topics.[1,53]

Structurally, the product obtained *via* the hydrazine-mediated reduction of graphene oxide is quite distinct from its precursor. Upon addition of hydrazine to the graphene oxide dispersion (typically performed at 80–100 °C), a black solid began to precipitate from suspension. This was likely a result of an increase in the hydrophobicity of the material caused by a decrease in the polar functionality on the surface of the platelet.[48] The BET surface area of the resulting material was measured to be 466 $m^2\ g^{-1}$; far below the theoretical value of fully exfoliated pristine graphene ($\sim$2620 $m^2\ g^{-1}$).[54] This could be due to incomplete exfoliation during sonication of the GO, but a second contributing factor may be generation of inaccessible surface caused by the agglomeration/precipitation during reduction. A C : O ratio of 10.3 : 1 was measured for reduced graphene oxide by

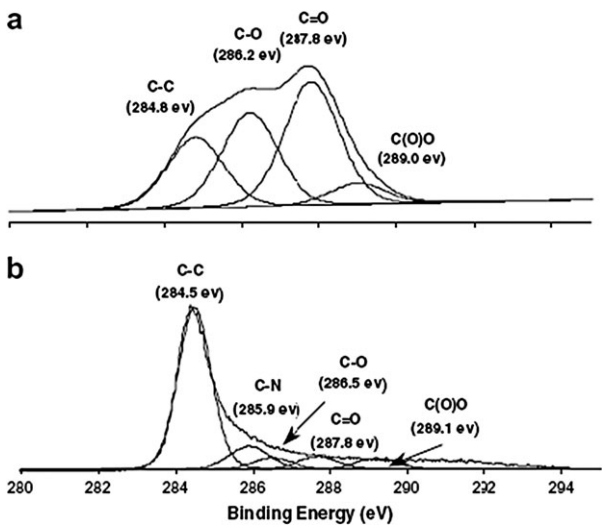

Fig. 8 The C-1s XPS spectra of: (a) graphene oxide, (b) hydrazine hydrate-reduced graphene oxide (from ref. 48).

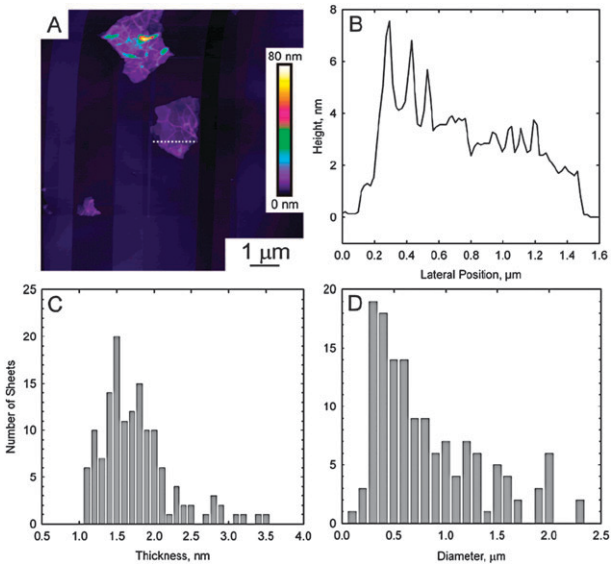

Fig. 9 (A) Contact-mode AFM scan of reduced graphene oxide deposited on a freshly cleaved pyrolytic graphite surface. (B) Height profile through the dashed line shown in part A. (C) Histogram of platelet thicknesses from images of 140 platelets. The mean thickness is 1.75 nm. (D) Histogram of diameters from the same 140 platelets. No correlation between diameter and thickness could be discerned (from ref. 61).

elemental analysis, compared with 2.7 : 1 for GO.[4813]C solid state MAS NMR spectroscopy also showed no discernible signals attributed to oxygen-containing groups; only a broad peak at $\delta = 117$ ppm , widely believed[25,28,36] to be attributable to alkenes of various types. Carbonyl, epoxy, and carboxylic acid signatures were detected in the XPS spectrum of the material (Fig. 8), but these are far diminished from their starting intensities, and were also dwarfed by the C–C and C=C signals. The powder conductivity (simply the bulk conductivity of a powderized sample) of the reduced sample was measured to be 2400 ± 200 S m^{-1}, compared with 2500 ± 20 S m^{-1} for graphite and 0.021 ± 0.002 S m^{-1} for GO.[48] Interestingly, the Raman spectra showed an increase in the D/G ratio of the reduced product; intuitively, a decrease in this ratio would be expected as the disorder associated with the amorphous graphene oxide diminishes. This experimental observation is suggested to be indicative of a decrease in the size of sp^2 domains upon reduction. The reason for such a decrease in size is not clear. One hypothesis is that reduction *via* hydrazine decreases the spatial dimensions of the sp^2 regions in the graphene, but increases their overall presence in the material, resulting in the observed increase in the conductivity. Similar results have been obtained through the use of anhydrous hydrazine as well.[3]

One of the disadvantages of using chemical methods of reduction, hydrazine in particular, is the introduction of heteroatomic impurities. While effective at removing oxygen functionality, nitrogen tends to remain covalently bound to the surface of graphene oxide, likely in the form of hydrazones, amines, aziridines or other similar structures (Table 1).[55] Residual C–N groups have a profound effect on the electronic structure of the resulting graphene, functioning as n-type dopants.[56] No simple route exists (*e.g.* hydrolysis, thermolysis, *etc.*) for removing these impurities, which can be present in C : N ratios as low as 16.1 : 1, as determined by elemental analysis.[48]

In a recent report, sodium borohydride ($NaBH_4$) was demonstrated to function more effectively than hydrazine as a reductant of graphene oxide (Table 1).[55] Though $NaBH_4$ is slowly hydrolyzed by water, this process is kinetically slow enough that freshly prepared solutions, having a large excess of reducing agent, still function effectively as reductants of graphene oxide. The scalability of such an approach, given its inherent inefficiencies, remains uncertain, however. $NaBH_4$ afforded materials with sheet resistances (R_{sh}) as low as 59 kΩ sq^{-1} (compared to 780 kΩ sq^{-1} for a hydrazine reduced sample, measured in the same study), and C : O ratios as high as 13.4 : 1 (compared to 6.2 : 1 for hydrazine). The use of borohydride has the additional advantage of introducing few, if any, heteroatoms to the graphene structure following reduction. Consistent with its demonstrated reactivity in other organic reactions, $NaBH_4$ is most effective at reducing C=O species, while having low to moderate efficacy in the reduction of epoxides and carboxylic acids. Additional alcohols are the principal impurities that are generated during this reductive process (as a result of the hydrolysis of the boronic ester). This is reflected in the relatively high heteroatom content of the C 1s peak in the XPS spectrum (13.4% for $NaBH_4$; 14.5% for hydrazine). The very low sheet resistance of these products suggests that heteroatom content may be a minor concern in producing useful graphene samples, however.

Other reductants have been used for the chemical formation of graphene including hydroquinone,[57] gaseous hydrogen (after thermal expansion),[58] and strongly alkaline solutions.[59,60] Reduction by hydrogen proved to be effective (C : O ratio of 10.8–14.9 : 1), while hydroquinone and alkaline solutions tend to be inferior to stronger reductants, such as hydrazine and sodium borohydride, based on semiquantitative results. Sulfuric acid or other strong acids can also be used to facilitate dehydration of the graphene surface.[37] For graphene structures that are contaminated with large amounts of alcohols (such as those obtained after borohydride reduction), this is a particularly useful workup procedure. The use of multiple chemical reductants has also been demonstrated as a route to rigorously reduced graphene,[47] though the benefit of this approach appears limited given the effectiveness of hydrazine and $NaBH_4$ on their own.

3.1.2 Thermally-mediated reduction. Chemical reduction is certainly the most common method of reducing graphene oxide, but it is by no means the only method. Results have been presented on the thermal exfoliation and reduction of GO.[61,62] Rather than using a chemical reductant to strip the oxide functionality from the surface, it is possible to create thermodynamically stable carbon oxide species by directly heating GO in a furnace.[60] Exfoliation of the stacked structure occurs through the extrusion of carbon dioxide§ generated by heating GO to 1050 °C. The high temperature gas creates

§ Carbon monoxide, water, and other small molecule hydrocarbons are also possible byproducts, but for their simulations Car and coworkers have assumed the extrusion product to be pure CO_2.[62]

Table 1 Sheet resistance and elemental composition of reduced graphene oxide films using $NaBH_4$ or N_2H_4 as the reducing agents (adapted from ref. 55)

$NaBH_4$			N_2H_2			
XPS			XPS			
Total elemental C : O ratio	Heterocarbon component of C-1s peak (%)	Sheet resistance ($k\Omega$ sq^{-1})	Total elemental C : O ratio	Heterocarbon component of C-1s peak (%)	N-1s peak intensity (%)	Sheet resistance ($k\Omega$ sq^{-1})
2.8	74.1	—	2.8	74.1	—	—
4.3	27.9	—	3.9	26.4	1.3	69 0000
4.9	16.2	79	4.5	19.0	2.1	12 000
5.3	13.4	59	5	18.6	2.6	3460
—	—	—	6.2	14.5	2.4	780

enormous pressure within the stacked layers. Based on state equations, a pressure of 40 MPa is generated at 300 °C, while as much as 130 MPa is generated at 1000 °C.[61] Evaluation of the Hamaker constant predicts that a pressure of only 2.5 MPa is necessary to separate two stacked graphene oxide platelets.[61] BET surface areas of 600–900 m^2 g^{-1} have been reported for this material (a methylene blue absorption method is also applied, giving a surface area of 1850 m^2 g^{-1}); roughly 80% of the platelets investigated by AFM are single platelets.[61]

A notable effect of thermal exfoliation is the structural damage caused to the platelets by the release of carbon dioxide.[63] Approximately 30% of the mass of the GO is lost during the exfoliation process, leaving behind vacancies and topological defects throughout the plane of the reduced graphene oxide platelet.[62] Defects inevitably affect the electronic properties of the product by decreasing the ballistic transport path length and introducing scattering sites. Despite these structural defects, however, bulk conductivities of 1000–2300 S m^{-1} were measured, indicating effective overall reduction and restoration of the planes' electronic structure. Although it has not been studied to date, these defects may also have an effect on the mechanical properties of the product, compared to a chemically-reduced sample.[64–66]

3.1.3 Electrochemical reduction. Another final method that shows promise for the reduction of graphene oxide relies on the electrochemical removal of the oxygen functionalities. Though chemically-reduced graphene oxide had previously been coated with metallic nanoparticles *via* electrodeposition, representing one of the few uses of CMGs in electrochemistry,[67] only recently has electrochemical reduction been used to alter the structure of graphene oxide or graphene itself.[68] In principle, this could avoid the use of dangerous reductants (*e.g.* hydrazine) and the need to dispose of the byproducts. After depositing thin films of graphene oxide on a variety of substrates (glass, plastic, ITO, *etc.*), electrodes were placed at opposite ends of the film and linear sweep voltammetry was run in a sodium phosphate buffer. Reduction began at −0.60 V and reached a maximum at −0.87 V. Rapid reduction was observed during the first 300 s, followed by a reduced rate of reduction up to 2000 s, and finally a decrease to background current levels up to 5000 s. Elemental analysis of the resultant material revealed a C : O ratio of 23.9 : 1; the conductivity of the film was measured to be approximately 8500 S m^{-1}. As with many of the aforementioned methods, the reduction mechanism remains unclear. The authors proposed the reaction pathway shown in Scheme 3, highlighting the crucial role of hydrogen ions in the buffer solution. Though this route appears to be extremely effective (and yet mild) at reducing the extant oxide functionality, and it precludes the need for hazardous chemical reactants and their byproducts, electrochemical reduction has not been demonstrated on a large sample. The deposition of reduced graphene oxide onto the electrodes is likely to render bulk electrochemical reduction difficult on a preparative scale. Scalability is a fundamental requirement of a useful synthetic protocol if graphene is to be broadly utilized.

3.2 Chemical functionalization

We have discussed removing oxygen functional groups (reduction) from graphene oxide platelets in the previous sections. In this section, we will discuss the addition of other groups to graphene oxide platelets using various chemical reactions that provide for either covalent or non-covalent attachment to the resulting chemically modified graphenes (CMGs). Such approaches, which add functionality to groups already present on the graphene oxide, render graphene/graphite oxide a more versatile precursor for a wide range of applications.

Graphene oxide platelets have chemically reactive oxygen functionality, such as carboxylic acid, groups at their edges (according to the widely accepted Lerf–Klinowski model), and epoxy and hydroxyl groups on the basal planes. An ideal approach to the chemical modification of graphene oxide would utilize orthogonal reactions of these groups to selectively functionalize one site over another. Demonstration of the selectivity of these chemical transformations remains challenging, however. In some instances, reaction with multiple functionalities is possible, and the wide range of chemical compositions present in the reactant known as "graphene oxide" makes isolation and rigorous characterization of the products practically impossible. Nevertheless, reactions involving individual functional groups found on graphene oxide will be discussed separately.

3.2.1 At the carboxylic acid group of graphene oxide. A wide range of reactions utilizing carboxylic acids has been

$$\underset{\text{Oxide}}{\text{Graphene}} + a\text{H}^+ + be^- \longrightarrow \underset{\text{Oxide}}{\text{Reduced Graphene}} + c\text{H}_2\text{O}$$

Scheme 3 Proposed reaction for the electrochemical reduction of graphene oxide in a sodium phosphate buffer (adapted from ref. 68).

developed over the course of the development of small molecule organic chemistry, and many of these reactions can be and have been applied to graphene oxide. The coupling reactions often require activation of the acid group using thionyl chloride ($SOCl_2$),[69–72] 1-ethyl-3-(3-dimethylaminopropyl)-carbodiimide (EDC),[73] *N*,*N*′-dicyclohexylcarbodiimide (DCC),[74] or 2-(7-aza-1*H*-benzotriazole-1-yl)-1,1,3,3-tetramethyluronium hexafluorophosphate (HATU).[75] Subsequent addition of nucleophilic species, such as amines or hydroxyls, produce covalently attached functional groups to graphene oxide platelets *via* the formation of amides or esters. The products are most often characterized by X-ray photoelectron (XP), Fourier transform infrared (FT-IR), and NMR spectroscopies.

Introduction of substituted amines is one of the most common methods of covalent functionalization, and the final products have been investigated for various applications in optoelectronics,[70–72] biodevices,[75] drug-delivery vehicles,[73] and polymer composites (see below).[74,76] As an example of the utility of these functionalized materials, the addition of long, aliphatic amine groups was demonstrated to increase the dispersability of chemically modified graphene platelets in organic solvents.[69] Likewise, porphyrin-functionalized primary amines and separately, fullerene-functionalized secondary amines have been attached to graphene oxide platelets (Fig. 10),[70–72] affording materials with useful nonlinear optical performance.

In addition to small molecules, polymers have also been attached to the surface of graphene oxide. These attachments are typically made by either grafting-onto or grafting-from approaches. The addition of an aliphatic diamine to EDC-activated graphene oxide produced amine-functionalized CMG platelets at the carboxylic acid groups. An atom transfer radical polymerization (ATRP) initiator, (α-bromoisobutyryl-bromide), was attached to the terminal amine, as well as the hydroxyl groups on the basal plane.[77,78] Polymers were then grown from the surface of the resulting material and afforded CMGs with increased dispersibility in many solvents, including water and methanol, depending on the monomer used (Fig. 11).[76] Using a grafting-onto approach, pre-formed poly(vinyl alcohol) (PVA) was attached to carbodiimide-activated carboxylic acid groups of graphene oxide platelets *via* ester

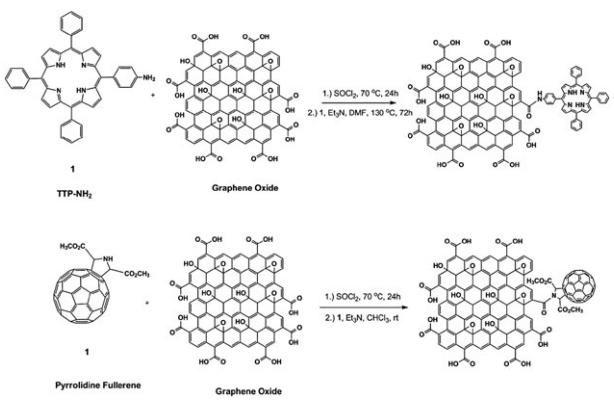

Fig. 10 Functionalization of the carboxylic acid groups of graphene oxide showing the covalent attachment of porphyrins and fullerenes (adapted from ref. 71).

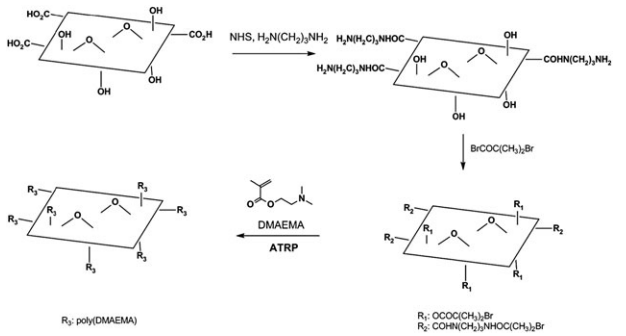

Fig. 11 Synthesis of PDMAEMA chains on graphene oxide by ATRP (adapted from ref. 76).

linkages.[74] The resulting polymer composite was well-dispersed in water and DMSO without further dispersion agents.

Aside from activation and amidation/esterification of the carboxyls on graphene oxide, it is also possible to convert them into other reactive groups. Stankovich and coworkers demonstrated that the generation of amide and carbamate ester groups from carboxylic acid and hydroxyl groups, respectively, of graphene oxide platelets could be achieved through the addition of isocyanate derivatives with various aliphatic and aromatic groups (Fig. 12).[79] The resulting CMG platelets were well dispersed in polar aprotic organic solvents.

3.2.2 At the epoxy group of graphene oxide. In addition to the carboxylic acids decorating the edges of graphene oxide, the platelets contain chemically reactive epoxy groups on their basal planes. The epoxy groups can be easily modified through ring-opening reactions under various conditions. A likely mechanism for this reaction involves nucleophilic attack at the α-carbon by the amine. As stated previously, multiple reactions may be occurring simultaneously: amine groups can react with carboxylic acid groups of graphene oxide through the amidation process previously discussed. A more detailed study differentiating these processes would be of great value to this field of research.

Wang and coworkers demonstrated the epoxide ring-opening reaction by the addition of octadecylamine to a dispersion of

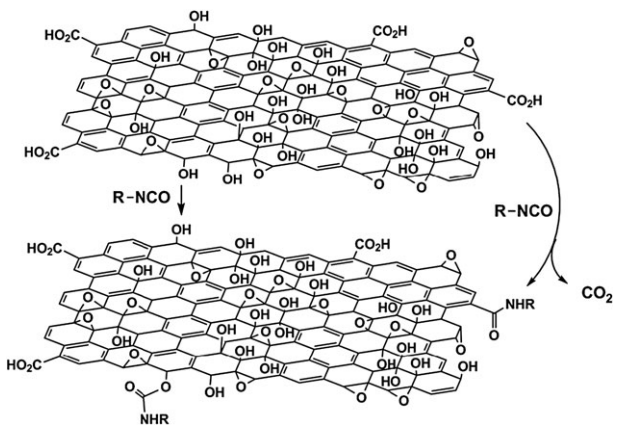

Fig. 12 Proposed reactions during the isocyanate treatment of graphene oxide (adapted from ref. 79).

graphene oxide, affording colloidal suspensions of CMG platelets in organic solvents.[80] The resulting suspensions were used for generation of thin CMG films by spin-casting or printing of the suspensions. The authors then thermally reduced the thin films and studied their electrical properties, demonstrating efficient reduction and the formation of high-quality, functionalized graphenes. In a related study, an ionic liquid (1-(3-aminopropyl)-3-methylimidazolium bromide; R-NH_2) with an amine end group was attached to graphene oxide platelets *via* the ring-opening reaction with epoxy groups (Fig. 13).[81] Due to the high polarity of the material, the resulting CMGs were well-dispersed in solvents such as water, DMF, and DMSO.

Reactions of the epoxy group of graphene oxide has also been used to stabilize solid-phase dispersions of CMGs. Yang and coworkers reported the covalent attachment of 3-amino-propyltriethoxysilane (APTS) to graphene oxide platelets.[82] The authors proposed that silane moieties are grafted *via* a nucleophilic S_N2 displacement reaction between the epoxide and the amine groups of APTS (Fig. 14). The mechanical properties of composite materials, composed of silica monoliths and the silane-functionalized graphene platelets, were enhanced by addition of the CMG. The authors suggested that this reinforcement can be induced by possible covalent bonding between the silica matrix and silane groups of the CMG platelets.

A final example of epoxide reactivity took its inspiration from the many examples of cross-linking reactions found in synthetic polymer chemistry. Poly(allylamine), which is a main chain aliphatic polymer with pendant amine groups (Fig. 15), was used to cross-link graphene oxide platelets *via* the epoxy groups of two or more platelets, stitching them together. The chemical cross-linking resulted in mechanical enhancement of 'paper-like' materials that are generated by simple filtration of colloidal suspensions of cross-linked CMG platelets.[64]

3.2.3 Non-covalent functionalization of graphene oxide. Graphene oxide can also exhibit non-covalent binding (*via* π–π stacking, cation-π or van der Waals interactions) on the sp^2 networks (where present) that are not oxidized or engaged in hydrogen bonding. Lu and coworkers reported a DNA sensor that utilized a non-covalent binding interaction between DNA or proteins and graphene oxide platelets,[83]

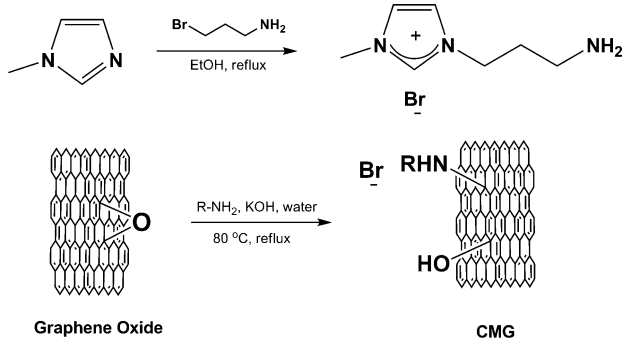

Fig. 13 Covalent functionalization of the epoxy groups of graphene oxide by an ionic liquid (R = 3-(3-methylimidazolium)propane), resulting in CMGs that were well-dispersed in polar media (adapted from ref. 81).

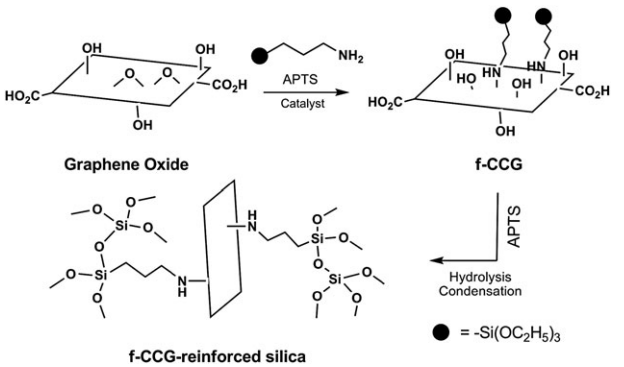

Fig. 14 Covalent functionalization of the epoxy groups of graphene oxide by silane groups, forming mechanically robust silica composites (adapted from ref. 80).

demonstrating that this material holds promise as a platform for sensitive and selective detection of DNA and/or proteins. A hybrid material of graphene oxide and doxorubicin hydrochloride (DXR) was also prepared *via* non-covalent interactions. The authors suggested π–π stacking, as well as hydrophobic interactions between the quinone functionality of DXR and sp^2 networks of graphene oxide, were the primary interactions that linked the two units together.[84] Also, the authors suggested that strong hydrogen bonding may be present between –OH and $–CO_2H$ groups of graphene oxide and –OH and $–NH_2$ groups in DXR.

3.2.4 Functionalization of reduced graphene oxide. Chemical or thermal reduction of graphene oxide platelets can restore the graphitic network in the basal plane of reduced graphene oxide platelets, as was discussed previously. Consequently, reduced graphene oxides have been frequently modified by non-covalent physisorption of both polymers[85–87] and small molecules[88,89]onto their basal planes *via* π–π stacking or van der Waals interactions. The authors of these studies suggested that adsorption of pyrene and derivatives thereof,[89,90] tetracyanoquinodimethane (TCNQ),[88] sulfonated poly(aniline) (SPANI),[86] perylene derivatives[90] and other aromatic species is likely caused by π–π stacking interactions. Alternatively, van der Waals interactions between electrostatically neutral, aliphatic copolymers and reduced graphene oxide was suggested as the driving force for the non-covalent adsorption observed in those system.[87] In the case of poly(styrene sulfonate) (PSS),[85] both π–π stacking and van der Waals interaction could lead to its adsorption.

Few examples of covalent functionalization of reduced graphene oxide exist. However, in one study, this type of bonding was reportedly achieved by reaction of reduced graphene oxide with diazonium salts (Fig. 16).[91] The resulting

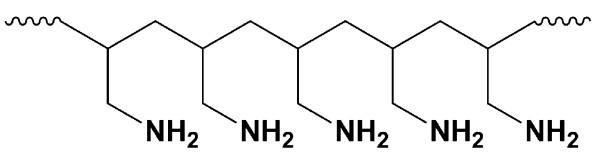

Fig. 15 Polyallylamine, which has been used to cross-link graphene oxide through the reaction with the epoxides of multiple platelets (adapted from ref. 64).

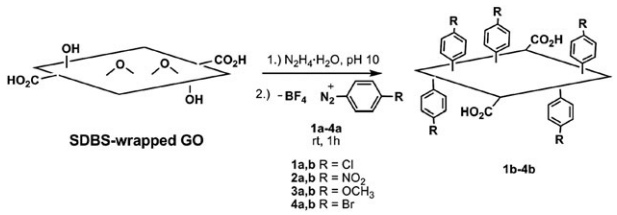

Fig. 16 Covalent functionalization of reduced graphene oxide platelets with diazonium salts (SDBS, sodium dodecylbenzenesulfonate) (adapted from ref. 90).

CMG platelets were readily dispersed in several polar organic solvents. Most covalent chemical modifications of graphene oxide previously discussed occurred at one or more of the various oxygen-containing functional groups present in graphene oxide. Hence, the reactivity observed in materials derived from the reduction of graphene oxide could be caused by residual functional groups left intact after incomplete reduction.

Conclusions and perspectives

In summary, graphene oxide has an extensive history that can be understood independent of its relationship to graphene. In addition to providing this historical perspective, we have presented an overview of GO and graphene oxide in their contemporary settings. Using flake graphite as a starting material, a variety of strong chemical oxidants have been used for the synthesis of graphene oxide, although its amorphous, berthollide composition has made understanding its true chemical structure an ongoing challenge. The most commonly accepted model remains the Lerf-Klinowski model, though others, such as the Dékány model, have been proposed as alternatives.

Among the most important chemical transformation of graphene oxide is its reduction to graphene-like materials. This can be achieved chemically through the use of strong reductants (such as hydrazine or sodium borohydride) thermally, or electrochemically. The resulting product is very similar to pristine graphene and has been used in a wide range of materials with potential physical and engineering applications. In addition to its reduction, however, graphene oxide is a useful platform for the fabrication of functionalized graphene platelets that can potentially confer improved mechanical, thermal and/or electronic properties. Both small molecules and polymers have been covalently attached to graphene oxide's highly reactive oxygen functionalities, or non-covalently attached on the graphitic surfaces of CMGs, for potential use in polymer composites, paper-like materials, sensors, photovoltaic applications, and drug-delivery systems.

A knowledge of graphene oxide's chemistry provides valuable insight into its reactivity and ultimately its properties, as well as those of graphenes that are derived therefrom. Much work remains to be done, however, in developing reliable characterization methods that will aid in unambiguous structural identification as well as synthetic procedures that lead to relatively uniform products. Finally, the development of reduction methods that minimize residual oxygen functionality will be of great value for large-scale synthetic preparations of graphene.

Acknowledgements

We gratefully acknowledge the Defense Advanced Research Projects Agency Carbon Electronics for RF Applications Center, the National Science Foundation (DMR-0907324), the Welch Foundation (F-1621) and the University of Texas at Austin for support.

Notes and references

1 A. K. Geim and K. S. Novoselov, *Nat. Mater.*, 2007, **6**, 183–191.
2 S. Park and R. S. Ruoff, *Nat. Nanotechnol.*, 2009, **4**, 217–224.
3 V. C. Tung, M. J. Allen, Y. Yang and R. B. Kaner, *Nat. Nanotechnol.*, 2009, **4**, 25–29.
4 H.-P. Boehm and E. Stumpp, *Carbon*, 2007, **45**, 1381–1383.
5 C. Schafheutl, *J. Prakt. Chem.*, 1840, **21**, 129–157.
6 C. Schafheutl, *Phil. Mag.*, 1840, **16**, 570–590.
7 B. C. Brodie, *Philos. Trans. R. Soc. London*, 1859, **149**, 249–259.
8 L. Staudenmaier, *Ber. Dtsch. Chem. Ges.*, 1898, **31**, 1481–1487.
9 W. S. Hummers and R. E. Offeman, *J. Am. Chem. Soc.*, 1958, **80**, 1339.
10 P. V. Lakshminarayanan, H. Toghiani and C. U. P. Jr, *Carbon*, 2004, **42**, 2433–2442.
11 N. Zhang, L.-y. Wang, H. Liu and Q.-K. Cai, *Surf. Interface Anal.*, 2008, **40**, 1190–1194.
12 F. A. Cotton, G. Wilkinson, C. A. Murillo and M. Bochmann, *Advanced Inorganic Chemistry*, Wiley India, Singapore, 2004.
13 K. R. Koch and P. F. Krause, *J. Chem. Ed.*, 1982, **59**, 973–974.
14 A. Simon, R. Dronskowski, B. Krebs and B. Hettich, *Angew. Chem., Int. Ed. Engl.*, 1987, **26**, 139–140.
15 M. Trömel and M. Russ, *Angew. Chem.*, 1987, **99**, 1037–1038.
16 M. Wissler, *J. Power Sources*, 2006, **156**, 142–150.
17 *USPTO*, ed. T. Ishikawa, T. Kanmaru, H. Teranishi and K. Onishi, Nippon Carbon Co., Ltd., USA, 1978.
18 U. Hofmann and R. Holst, *Ber. Dtsch. Chem. Ges. B*, 1939, **72**, 754–771.
19 G. Ruess, *Monatsh. Chem.*, 1946, **76**, 381–417.
20 M. Mermoux, Y. Chabre and A. Rousseau, *Carbon*, 1991, **29**, 469–474.
21 M. Dubois, J. Giraudet, K. Guerin, A. Hamwi, Z. Fawal, P. Pirotte and F. Masin, *J. Phys. Chem. B*, 2006, **110**, 11800–11808.
22 W. Scholz and H. P. Boehm, *Z. Anorg. Allg. Chem.*, 1969, **369**, 327–340.
23 T. Nakajima, A. Mabuchi and R. Hagiwara, *Carbon*, 1988, **26**, 357–361.
24 T. Nakajima and Y. Matsuo, *Carbon*, 1994, **32**, 469–475.
25 H. He, T. Riedl, A. Lerf and J. Klinowski, *J. Phys. Chem.*, 1996, **100**, 19954–19958.
26 A. Lerf, H. He, M. Forster and J. Klinowski, *J. Phys. Chem. B*, 1998, **102**, 4477–4482.
27 T. Szabo, O. Berkesi, P. Forgo, K. Josepovits, Y. Sanakis, D. Petridis and I. Dekany, *Chem. Mater.*, 2006, **18**, 2740–2749.
28 A. Lerf, H. He, T. Riedl, M. Forster and J. Klinowski, *Solid State Ionics*, 1997, **101–103**, 857–862.
29 A. Buchsteiner, A. Lerf and J. Pieper, *J. Phys. Chem. B*, 2006, **110**, 22328–22338.
30 A. Lerf, A. Buchsteiner, J. Pieper, S. Schöttl, I. Dekany, T. Szabo and H. P. Boehm, *J. Phys. Chem. Solids*, 2006, **67**, 1106–1110.
31 H. P. Boehm and W. Scholz, *Z. Anorg. Allg. Chem.*, 1965, **335**, 74–79.
32 D. Hadzi and A. Novak, *Faraday Trans.*, 1955, **51**, 1514.
33 A. M. Rodriguez and P. S. V. Jimenez, *Carbon*, 1986, **24**, 163.
34 H. He, J. Klinowski, M. Forster and A. Lerf, *Chem. Phys. Lett.*, 1998, **287**, 53–56.
35 U. Hofmann, A. Frenzel and E. Csalan, *Justus Liebigs Ann. Chem.*, 1934, **510**, 1.
36 W. Cai, R. D. Piner, F. J. Stadermann, S. Park, M. A. Shaibat, Y. Ishii, D. Yang, A. Velamakanni, S. J. An, M. Stoller, J. An, D. Chen and R. S. Ruoff, *Science*, 2008, **321**, 1815–1817.

37 W. Gao, L. B. Alemany, L. Ci and P. M. Ajayan, *Nat. Chem.*, 2009, **1**, 403–408.
38 T. Szabo, O. Berkesi and I. Dekany, *Carbon*, 2005, **43**, 3186–3189.
39 T. Szabo, E. Tombacz, E. Illes and I. Dekany, *Carbon*, 2006, **44**, 537–545.
40 D. W. Boukhvalov and M. I. Katsnelson, *J. Am. Chem. Soc.*, 2008, **130**, 10697–10701.
41 J. I. Paredes, S. Villar-Rodil, A. Martinez-Alonso and J. M. D. Tascon, *Langmuir*, 2008, **24**, 10560–10564.
42 H. A. Becerril, J. Mao, Z. Liu, R. M. Stoltenberg, Z. Bao and Y. Chen, *ACS Nano*, 2008, **2**, 463–470.
43 C. Gomez-Navarro, R. T. Weitz, A. M. Bittner, M. Scolari, A. Mews, M. Burghard and K. Kern, *Nano Lett.*, 2007, **7**, 3499–3503.
44 S. Stankovich, D. A. Dikin, G. H. B. Dommett, K. M. Kohlhaas, E. J. Zimney, E. A. Stach, R. D. Piner, S. T. Nguyen and R. S. Ruoff, *Nature*, 2006, **442**, 282–286.
45 Z. Li, W. Zhang, Y. Luo, J. Yang and J. G. Hou, *J. Am. Chem. Soc.*, 2009, **131**, 6320–6321.
46 L. Zhang, J. Liang, Y. Huang, Y. Ma, Y. Wang and Y. Chen, *Carbon*, 2009, **47**, 3365–3380.
47 Y. Si and E. T. Samulski, *Nano Lett.*, 2008, **8**, 1679–1682.
48 S. Stankovich, D. A. Dikin, R. D. Piner, K. A. Kohlhaas, A. Kleinhammes, Y. Jia, Y. Wu, S. T. Nguyen and R. S. Ruoff, *Carbon*, 2007, **45**, 1558–1565.
49 K. S. Novoselov, A. K. Geim, S. V. Morozov, D. Jiang, Y. Zhang, S. V. Dubonos, I. V. Grigorieva and A. A. Firsov, *Science*, 2004, **306**, 666–669.
50 F. A. Carey and R. J. Sundberg, in *Advanced Organic Chemistry Part B: Reactions and Synthesis*, Springer, New York, 2007, pp. 367–471.
51 S. Brunauer, P. H. Emmett and E. Teller, *J. Am. Chem. Soc.*, 1938, **60**, 309–319.
52 A. Das, B. Chakraborty and A. K. Sood, *Bull. Mater. Sci.*, 2008, **31**, 579–584.
53 J. H. Warner, M. H. Rümmeli, L. Ge, T. Gremming, B. Montanari, N. M. Harrison, B. Büchner and G. A. D. Briggs, *Nat. Nanotechnol.*, 2009, **4**, 500–504.
54 H. K. Chae, D. Y. Siberio-Perez, J. Kim, Y. Go, M. Eddaoudi, A. J. Matzger, M. O'Keeffe and O. M. Yaghi, *Nature*, 2004, **427**, 523–527.
55 H.-J. Shin, K. K. Sim, A. Benayad, S.-M. Yoon, H. K. Park, I.-S. Jung, M. H. Jin, H.-K. Jeong, J. M. Kim, J.-Y. Choi and Y. H. Lee, *Adv. Funct. Mater.*, 2009, **19**, 1987–1992.
56 S. J. Kanh, C. Kocabas, T. Ozel, M. Shim, N. Pimparkar, M. A. Alam, S. V. Rotkin and J. A. Rogers, *Nat. Nanotechnol.*, 2007, **2**, 230–236.
57 G. Wang, J. Yang, J. Park, X. Gou, B. Wang, H. Liu and J. Yao, *J. Phys. Chem. C*, 2008, **112**, 8192–8195.
58 Z.-S. Wu, W. Ren, L. Gao, B. Liu, C. Jiang and H.-M. Cheng, *Carbon*, 2009, **47**, 493–499.
59 X. Fan, W. Peng, Y. Li, X. Li, S. Wang, G. Zhang and F. Zhang, *Adv. Mater.*, 2008, **20**, 4490–4493.
60 H. P. Boehm, A. Clauss, G. O. Fischer and U. Hofmann, *Z. Anorg. Allg. Chem.*, 1962, **316**, 119–127.
61 M. J. McAllister, J.-L. Li, D. H. Adamson, H. C. Schniepp, A. A. Abdala, J. Liu, M. Herrera-Alonso, D. L. Milius, R. Car, R. K. Prud'homme and I. A. Aksay, *Chem. Mater.*, 2007, **19**, 4396–4404.
62 H. C. Schniepp, J.-L. Li, M. J. McAllister, H. Sai, M. Herrera-Alonso, D. H. Adamson, R. K. Prud'homme, R. Car, D. A. Saville and I. A. Aksay, *J. Phys. Chem. B*, 2006, **110**, 8535–8539.
63 K. N. Kudin, B. Ozbas, H. C. Schniepp, R. K. Prud'homme, I. A. Aksay and R. Car, *Nano Lett.*, 2008, **8**, 36–41.
64 S. Park, D. A. Dikin, S. T. Nguyen and R. S. Ruoff, *J. Phys. Chem. C*, 2009, **113**, 15801–15804.
65 S. Park, K.-S. Lee, G. Bozoklu, W. Cai, S. T. Nguyen and R. S. Ruoff, *ACS Nano*, 2008, **2**, 572–578.
66 J. T. Robinson, M. Zalalutdinov, J. W. Baldwin, E. S. Snow, Z. Wei, P. Sheehan and B. H. Houston, *Nano Lett.*, 2008, **8**, 3441–3445.
67 R. S. Sundaram, C. Gomez-Navarro, K. Balasubramanian, M. Burghard and K. Kern, *Adv. Mater.*, 2008, **20**, 3050–3053.
68 M. Zhou, Y. Wang, Y. Zhai, J. Zhai, W. Ren, F. Wang and S. Dong, *Chem.–Eur. J.*, 2009, **15**, 6116–6120.
69 S. Niyogi, E. Bekyarova, M. E. Itkis, J. L. McWilliams, M. A. Hamon and R. C. Haddon, *J. Am. Chem. Soc.*, 2006, **128**, 7720–7721.
70 Y. Xu, Z. Liu, X. Zhang, Y. Wang, J. Tian, Y. Huang, Y. Ma, X. Zhang and Y. Chen, *Adv. Mater.*, 2009, **21**, 1–5.
71 Z.-B. Liu, Y.-F. Xu, X.-Y. Zhang, X.-L. Zhang, Y.-S. Chen and J.-G. Tian, *J. Phys. Chem. B*, 2009, **113**, 9681–9686.
72 X. Zhang, Y. Huang, Y. Wang, Y. Ma, Z. Liu and Y. Chen, *Carbon*, 2009, **47**, 334–337.
73 Z. Liu, J. T. Robinson, X. Sun and H. Dai, *J. Am. Chem. Soc.*, 2008, **130**, 10876–10877.
74 L. M. Veca, F. Lu, M. J. Meziani, L. Cao, P. Zhang, G. Qi, L. Qu, M. Shrestha and Y.-P. Sun, *Chem. Commun.*, 2009, 2565–2567.
75 N. Mohanty and V. Berry, *Nano Lett.*, 2008, **8**, 4469–4476.
76 Y. Yang, J. Wang, J. Zhang, J. Liu, X. Yang and H. Zhao, *Langmuir*, 2009, **25**, 11808–11814.
77 M. Fang, K. Wang, H. Lu, Y. Yang and S. Nutt, *J. Mater. Chem.*, 2009, **19**, 7098–7105.
78 S. H. Lee, D. R. Dreyer, J. An, A. Velamakanni, R. D. Piner, S. Park, Y. Zhu, S. O. Kim, C. W. Bielawski and R. S. Ruoff, *Macromol. Rapid Commun.*, 2009, DOI: 10.1002/marc.200900641.
79 S. Stankovich, R. Piner, S. T. Nguyen and R. S. Ruoff, *Carbon*, 2006, **44**, 3342–3347.
80 S. Wang, P.-J. Chia, L.-L. Chua, L.-H. Zhao, R.-Q. Png, S. Sivaramakrishnan, M. Zhou, R. G.-S. Goh, R. H. Friend, A. T. S. Wee and P. K.-H. Ho, *Adv. Mater.*, 2008, **20**, 3440–3446.
81 H. Yang, C. Shan, F. Li, D. Han, Q. Zhang and L. Niu, *Chem. Commun.*, 2009, 3880–3882.
82 H. Yang, F. Li, C. Shan, D. Han, Q. Zhang, L. Niu and A. Ivaska, *J. Mater. Chem.*, 2009, **19**, 4632–4638.
83 C.-H. Lu, H.-H. Yang, C.-L. Zhu, X. Chen and G.-N. Chen, *Angew. Chem., Int. Ed.*, 2009, **48**, 4785–4787.
84 X. Yang, X. Zhang, Z. Liu, Y. Ma, Y. Huang and Y. Chen, *J. Phys. Chem. C*, 2008, **112**, 17554–17558.
85 S. Stankovich, R. Piner, X. Chen, N. Wu, S. T. Nguyen and R. S. Ruoff, *J. Mater. Chem.*, 2006, **16**, 155–158.
86 H. Bai, Y. Xu, L. Zhao, C. Li and G. Shi, *Chem. Commun.*, 2009, 1667–1669.
87 S.-Z. Zu and B.-H. Han, *J. Phys. Chem. C*, 2009, **113**, 13651–13657.
88 R. Hao, W. Qian, L. Zhang and Y. Hou, *Chem. Commun.*, 2008, 6576–6578.
89 Y. Xu, H. Bai, G. Lu, C. Li and G. Shi, *J. Am. Chem. Soc.*, 2008, **130**, 5856–5857.
90 Q. Su, S. Pang, V. Alijani, C. Li, X. Feng and K. Müllen, *Adv. Mater.*, 2009, **21**, 3191–3195.
91 J. R. Lomeda, C. D. Doyle, D. V. Kosynkin, W.-F. Hwang and J. M. Tour, *J. Am. Chem. Soc.*, 2008, **130**, 16201–16206.